Accurate ab initio energetics of extended systems via explicit correlation embedded in a density functional environment

N. Govind, Y.A. Wang, A.J.R. da Silva, E.A. Carter [*]

Department of Chemistry and Biochemistry, Box 951569, University of California, Los Angeles, CA 90095-1569, USA

Abstract

We present a new embedding technique that combines density functional theory (DFT) and explicit electron-correlation techniques. We construct a periodic-DFT-based embedding potential as a local one-electron operator within more accurate electron-correlation calculations. We demonstrate how DFT calculations can be systematically improved via this procedure. We benchmark the method against nearly exact calculations with a simple model of Li_2Mg_2 and further corroborate it with an application to the experimentally well studied $CO/Cu(111)$ system. Our results are in good agreement with near-full configuration interaction (CI) calculations in the former case and experimental adsorbate binding energies in the latter. © 1998 Published by Elsevier Science B.V. All rights reserved.

1. Introduction

Interactions of atoms and molecules with surfaces have been studied over the last two decades using a number of established theoretical techniques. They can be divided into three basic categories: finite cluster quantum chemistry (QC), periodic slab and Green's function DFT and embedded cluster (EC) methods. Traditional finite cluster QC can be accurate but implicitly relies on the localized nature of the interaction and consequently can suffer from edge artifacts. In addition, these methods cannot be applied to extended systems because of their prohibitive scaling properties. Periodic DFT calculations on the other hand are relatively inexpensive and can handle infinite systems by virtue of their construction [1]. They are however limited by the local density approximation (LDA) treatment of the exchange-correlation effects [2], which is accurate in predicting structures but can be quite wrong for binding energies [3]. Although nonlocal corrections via the generalized gradient approximation (GGA) [4] sometimes improves the situation [5], a general convergence rule does not exist [6]. The Green's function [7] technique has also been used successfully to study adsorbate-surface problems. Like the periodic slab scheme, this yields a proper description of the bulk and surface states, but is also hampered by the LDA/GGA descriptions of the exchange-correlation effects. EC methods are advantageous as they have the capacity of preserving the strengths of finite cluster QC while accounting for the presence of the rest of the system consistently within one framework. This idea has been implemented in vari-

_____

[*] Corresponding author. E-mail: eac@chem.ucla.edu

ous forms [8–17]. However, they utilize arbitrary orbital localization procedures and have other shortcomings, including limited levels of theory (mainly at the Hartree–Fock or the Kohn–Sham level) for the strong interaction region. Explicit correlation has been introduced before, but always with either semiempirical [14] or somewhat unphysical embedding environments [13,15].

2. Formalism

We present a new embedding procedure that utilizes the strengths of both cluster and slab models. The method treats the extended parts of the system within periodic DFT and the embedded cluster (adsorbate and a few surface atoms), within explicit ab initio correlation methods. We thus partition the system into regions where the best suited methods can be applied (see Fig. 1). Region I, the adsorbate-surface region, is treated with QC and Region II, the surface/bulk background, is treated with periodic DFT. Region I is chosen large enough to account for surface-adsorbate interactions, but small enough to allow high-level ab initio calculations. The influence of Region II on Region I is brought in by a local one-electron embedding potential $v_{emb}(r)$.

The basic problem one needs to solve is

$$E_{tot} = \left\langle \Psi_{tot} | \hat{H}_I + \hat{H}_{II} + \hat{H}_{int} | \Psi_{tot} \right\rangle, \tag{1}$$

where Ψ_{tot} is a normalized many-body wavefunction of the total system, $\hat{H}_I$ and $\hat{H}_{II}$ are the subsystem Hamiltonians and $\hat{H}_{int}$ is the interaction Hamilto-
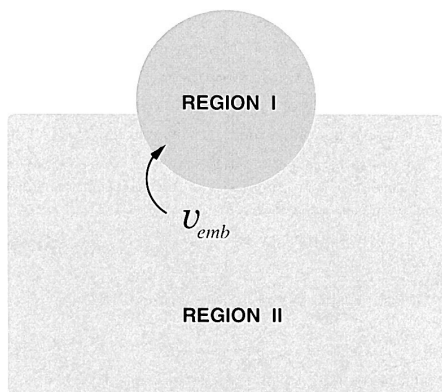
nian. This equation poses a serious problem because it deals with the total wavefunction of an infinite system, which is beyond the reach of any conventional ab initio method. However with the partitioning introduced in Fig. 1, the total energy, E_{tot}, can be written formally as

$$E_{tot} = E_I + E_{II} + E_{int}, \tag{2}$$

where in the language of DFT, E_I, E_{II} and E_{tot} all have the similar expression

$$E_i = T_s[\rho_i] + V_{ne}^i[\rho_i] + J[\rho_i] + E_{xc}[\rho_i] + V_{nn}^i, \tag{3}$$

with $i =$ I, II, tot. Here, T_s, V_{ne}, J, E_{xc} and V_{nn} are the non-interacting kinetic, electron-nuclear attraction (including pseudopotentials), electron–electron repulsion, exchange-correlation and nuclear–nuclear repulsion energy functionals, respectively. The interaction piece is then defined as

$$E_{int} = T_s^{int} + E_{xc}^{int} + V_{ne}^{int} + J^{int} + V_{nn}^{int}, \tag{4}$$

where terms on the right-hand side (RHS) are given by

$$T_s^{int} = T_s[\rho_{tot}] - T_s[\rho_I] - T_s[\rho_{II}], \tag{5}$$

$$E_{xc}^{int} = E_{xc}[\rho_{tot}] - E_{xc}[\rho_I] - E_{xc}[\rho_{II}], \tag{6}$$

$$V_{ne}^{int} = V_{ne}^{tot}[\rho_{tot}] - V_{ne}^I[\rho_I] - V_{ne}^{II}[\rho_{II}]$$
$$= \left\langle v_{ne}^I | \rho_{II} \right\rangle + \left\langle v_{ne}^{II} | \rho_I \right\rangle, \tag{7}$$

$$J^{int} = J[\rho_{tot}] - J[\rho_I] - J[\rho_{II}] = \left\langle \rho_I | r_{12}^{-1} | \rho_{II} \right\rangle, \tag{8}$$

$$V_{nn}^{int} = V_{nn}^{tot} - V_{nn}^I - V_{nn}^{II}. \tag{9}$$

Here, E_{xc} is handled at the DFT level and T_s is approximated by well tested functionals. The choice and utility of the T_s functionals are based on a detailed study for atoms, solids, and solid surfaces [18].

$v_{emb}(r)$ can now be constructed from Eq. (4), by performing a functional derivative with respect to ρ_I,

$$v_{emb}(r) = \frac{\delta E_{int}}{\delta \rho_I} = \frac{\delta T_s^{int}}{\delta \rho_I} + \frac{\delta E_{xc}^{int}}{\delta \rho_I} + \frac{\delta V_{ne}^{int}}{\delta \rho_I}$$
$$+ \frac{\delta J^{int}}{\delta \rho_I}, \tag{10}$$

REGION I

v_{emb}

REGION II

Fig. 1. Partitioning of the system.

where terms on the RHS are given by

$$\frac{\delta T_{\text{s}}^{\text{int}}}{\delta \rho_{\text{I}}} = \frac{\delta T_{\text{s}}[\rho_{\text{tot}}]}{\delta \rho_{\text{tot}}} - \frac{\delta T_{\text{s}}[\rho_{\text{I}}]}{\delta \rho_{\text{I}}} , \quad (11)$$

$$\frac{\delta E_{\text{xc}}^{\text{int}}}{\delta \rho_{\text{I}}} = \frac{\delta E_{\text{xc}}[\rho_{\text{tot}}]}{\delta \rho_{\text{tot}}} - \frac{\delta E_{\text{xc}}[\rho_{\text{I}}]}{\delta \rho_{\text{I}}} , \quad (12)$$

$$\frac{\delta V_{\text{ne}}^{\text{int}}}{\delta \rho_{\text{I}}} = v_{\text{ne}}^{\text{II}}(\boldsymbol{r}) , \quad (13)$$

$$\frac{\delta J^{\text{int}}}{\delta \rho_{\text{I}}} = \int \frac{\rho_{\text{tot}}(\boldsymbol{r}') - \rho_{\text{I}}(\boldsymbol{r}')}{|\boldsymbol{r} - \boldsymbol{r}'|} d\tau' . \quad (14)$$

Here we have assumed that ρ_{I} and ρ_{II} are independent functions. Since ρ_{tot} obtained in DFT is a good representation to the true total density, we do not need to update ρ_{tot}. This implies that the variational domain is

$$\{ \rho_{\text{I}}, \rho_{\text{II}} \mid \rho_{\text{I}} + \rho_{\text{II}} \equiv \rho_{\text{tot}} \}, \quad (15)$$

which means that during the search of the variational stationary point, both ρ_{I} and ρ_{II} are varied simultaneously with fixed ρ_{tot}, although only ρ_{I} is explicitly optimized.

The algorithm constitutes the following steps:

1. The Kohn–Sham equations are solved for the total system via a standard pseudopotential plane-wave supercell DFT calculation, which yields ρ_{tot}.
2. ρ_{I} is calculated using quantum chemistry methods, and $v_{\text{emb}}(\boldsymbol{r})$ is then obtained.
3. $v_{\text{emb}}(\boldsymbol{r})$ is inserted in Step 2 as an effective local one-electron operator in a quantum-chemistry code and ρ_{I} is updated to self-consistency.

The construction of $v_{\text{emb}}(\boldsymbol{r})$ is done in reciprocal space for portions involving ρ_{tot}, while the terms involving ρ_{I} are evaluated in real space on a very fine uniform grid.

The scheme was implemented with the plane-wave DFT code, CASTEP [1] for the DFT and a modified QC code, HONDO [19] for the ab initio calculations.

The role of our embedding is revealed succinctly by rewriting E_{tot} as

$$\begin{aligned} E_{\text{tot}}^{\text{emb}} &= E_{\text{I}}^{\text{ab}} + E_{\text{II}}^{\text{DFT}} + E_{\text{int}}^{\text{DFT}} \\ &= \left(E_{\text{I}}^{\text{DFT}} + E_{\text{II}}^{\text{DFT}} + E_{\text{int}}^{\text{DFT}} \right) + \left(E_{\text{I}}^{\text{ab}} - E_{\text{I}}^{\text{DFT}} \right) \\ &= E_{\text{tot}}^{\text{DFT}} + \Delta E_{\text{I}}^{\text{emb}} , \end{aligned} \quad (16)$$

where the superscripts denote which method applies. This shows that the ab initio treatment of Region I improves the DFT result by correcting the DFT energy for the total system. This procedure should help systematically remedy the LDA/GGA description of the exchange-correlation effects used in conventional DFT.

Our embedding scheme brings together the merits and eliminates deficiencies of various methods [1,7–17]. First, QC methods, used to optimize ρ_{I}, provide very accurate energetics in a systematic manner. Second, all components of $v_{\text{emb}}(\boldsymbol{r})$ are expressed purely in terms of ρ_{tot} and ρ_{I}, where only the latter is updated and the former is kept fixed. Third, the correct periodic boundary conditions are used, as ρ_{tot} is calculated using a supercell DFT calculation. The resulting potentials and densities (ρ_{tot} and ρ_{I}) are continuous across the interface between Regions I and II. Fourth, an orbital localization in Region I is not needed. Fifth, an indented crystal for Region II as employed by Abarenkov et al. [15] is not used, eliminating consequent density artifacts. Sixth, a semiempirical embedding potential is not used. The only arbitrariness lies in the choice of the energy density functionals employed in $v_{\text{emb}}(\boldsymbol{r})$: they are not known exactly and suitable approximations must be made. We have observed that the choice of T_{s} is critical and must be chosen carefully. A detailed analysis of various T_{s} functionals will be published elsewhere [18].

3. Applications

3.1. Toy model: $Li_2 Mg_2$

The initial test was performed on a toy model [15]. This model was considered so that the scheme could be gauged against near-full CI (nFCI) results. We examined the binding energy of Li_2 to Mg_2 in a linear geometry, with $R_{Li_2} = 3.465$ Å, $R_{Mg_2} = 2.543$ Å, and the closest $R_{LiMg} = 3.002$ Å. Li_2 and the Mg closest to it comprised Region I and the remaining Mg comprised Region II. This is a meaningful partitioning, as one can think of the Li_2Mg as the embedded cluster and the lone Mg as the embedding region.

ρ_{tot} was calculated using CASTEP with standard norm-conserving pseudopotentials [20]. A suitable cutoff (300 eV) and a supercell large enough (10 Å × 10 Å × 30 Å) to prevent interactions with neighboring cells were used. Both LDA [2] and GGA [4] densities were calculated. A fine enough grid was also used to represent the densities properly. ρ_{I} was calculated using HONDO at the spin-restricted Hartree–Fock (RHF), 2nd-order, 3rd-order, and 4th-order Møller–Plesset perturbation theory (MP2, MP3, and MP4) levels, under the influence of $v_{\text{emb}}(\mathbf{r})$. Standard contracted Gaussian bases (CGTO) $(4s,4p)/[2s,2p]$ were used for Li and Mg along with their respective pseudopotentials [21], so that full CI (FCI) calculations could be performed on the isolated Li$_2$ and Mg$_2$ fragments and a large-scale multi-reference singles and doubles CI calculation (MRSDCI), on the total system. The iterative natural orbital approach [22] was taken for the MRSDCI calculation using the MELD programs [23], until the CI energy did not change at the 6th decimal point with increasing size of the CI Hamiltonian matrix. The final MRSDCI has a dimension of 380153 (about one-third of its FCI size), and should be very close to the FCI limit and will be denoted as the nFCI calculation. GHOST functions were used to implement the Boys counterpoise correction to the basis set superposition error [24] and to produce the correct tails of ρ_{I} around the surface atom nuclei [13]. The T_s contribution to $v_{\text{emb}}(\mathbf{r})$ was calculated numerically using the Thomas–Fermi model [6] while its contribution to $E_{\text{I}}^{\text{DFT}}$ and $E_{\text{tot}}^{\text{DFT}}$ was calculated using the Thomas–Fermi– $\frac{1}{9}$von Weizsäcker model [6]. The von Weizsäcker contribution was eliminated from $v_{\text{emb}}(\mathbf{r})$ due to numerical instabilities. Similar models have been shown to give a good description of small clusters [25]. The choice of T_s is critical and has been chosen properly [18].

The results are summarized on the left hand side of Table 1. Both the LDA and the GGA overbind the system by nearly four times when compared to nFCI. The embedding helps decrease the overbinding systematically as the level of theory is increased. In particular, the binding energy is reproduced to within 0.007 eV of nFCI when the embedding is performed at the MP4/LDA level. Also, note that including the GGA does not greatly improve on the LDA embedding results.

Table 1
Binding energies (in eV) for the linear Li$_2$Mg$_2$ and CO/Cu(111)

Method		Li$_2$Mg$_2$	CO/Cu(111)
Pure DFT	LDA-Cluster	−0.5501	−1.2138
	GGA-Cluster	−0.5264	−1.1834
	LDA-Slab		−0.8406
	GGA-Slab		−0.7682
Finite cluster	RHF	−0.1121	−0.4288
	MP2	−0.1815	−1.5973
	MP3	−0.1755	−0.9720
	MP4	−0.1729	−2.1585
	nFCI [a]/Expt. [b]	−0.1565	−0.52
Embedded cluster [c]	RHF/LDA	−0.3052	−0.7895
	MP2/LDA	−0.2027	−0.7102
	MP3/LDA	−0.1654	−0.6824
	MP4/LDA	−0.1501	−0.6639
	RHF/GGA	−0.2816	−0.7271
	MP2/GGA	−0.1790	−0.7030
	MP3/GGA	−0.1517	−0.6891
	MP4/GGA	−0.1378	−0.6823

[a] The near-full CI result for the linear Li$_2$Mg$_2$. [b] The experimental value for CO/Cu(111). [c] QC method for cluster region listed first, DFT method for background listed last.

3.2. CO / Cu(111)

We next studied the CO/Cu(111) system whose adsorbate binding energy and binding site are well known experimentally. Since our embedding scheme is ideally suited to examine low coverages, we set up our calculation to study a CO coverage of 0.125 monolayers. Infrared and isosteric heat of adsorption data [26] reveal atop CO and a binding energy of −0.52 eV at this coverage. The supercell (5.06 Å × 8.76 Å × 22.00 Å) was a slab containing 32 Cu atoms (8 atoms per layer) with 1 CO placed at an atop Cu site at the cell center. The chemisorption region was a cluster containing the CO molecule at the atop site with the 3 Cu atoms closest beneath the surface Cu atom (the smallest tetrahedral Cu$_4$ unit of the (111) surface). The geometry was optimized at the LDA level ($R_{\text{CO}} = 1.150$ Å, $R_{\text{CCu}} = 1.910$ Å), with the Cu slab fixed at its bulk structure.

ρ_{tot} was converged using a cutoff of 850 eV with integrations over the surface Brillouin zone (BZ) performed on a discrete mesh of 8 $\mathbf{k}$-points symmetrized over the irreducible BZ. A Gaussian broadening [27] of 0.25 eV was also used. ρ_{I} was cal-

culated within HONDO using two $(9s,5p,1d)/[3s,2p,1d]$ CGTO basis sets for C and O [28] and a $(5s,5p,5d)/[3s,3p,2d]$ CGTO basis set for Cu [29] (for C and O, see Ref. [21]), respectively, and suitable pseudopotentials [29] (the d-electrons were not pseudised). A ghost function [13], an optimized Cu $4s$ atomic orbital, was placed on each of the 12 closest Cu atoms around the Cu_4 unit. The T_s contributions to Eq. (11) in this case were treated differently in Regions I and II. The slab was treated with the Perrot functional [30] and the embedded cluster via the Zhao–Levy–Parr (ZLP) functional [31,32]. The Perrot functional by construction has the correct linear response properties for a nearly free electron gas and has been successfully tested in first principles simulations of bulk Na and Al [33]. In our case, this functional is only used to treat the Cu substrate, which can be thought of as being close to a 'nearly free electron' system. The ZLP functional has been shown to yield good results for small clusters [16].

The results of these calculations are summarized in the right half of Table 1. The embedding in this case not only decreases the overbinding compared with the DFT slab result, but also removes the oscillations in the binding energies seen in pure finite cluster QC calculations, emphasizing the importance of the correct treatment of Region II. The final MP4/LDA prediction is within 0.15 eV of experiment. Again, including the GGA does not greatly improve on the LDA embedding results.

4. Conclusion

We have developed a new embedding scheme for extended systems and have demonstrated its utility by applying it to a toy model and a real system. Binding energies were calculated using this scheme at the Møller–Plesset perturbation theory up to 4th order and the results are close to the exact or experimental values. This method represents a means to systematically improve DFT predictions, and is expected to be applicable to metallic, ionic, and molecular condensed phases. The method as it stands now can be extended to other high-order ab initio methods including MRSDCI, multi-configurational SCF, and multi-configurational MP2. This is under intense

study and will be addressed in future publications [18].

References

[1] M.C. Payne, M.P. Teter, D.C. Allan, T.A. Arias, J.D. Joannopoulos, Rev. Mod. Phys. 64 (1992) 1045.
[2] J.P. Perdew, A. Zunger, Phys. Rev. B 23 (1981) 5048.
[3] For example, P. Fulde, Electron Correlations in Molecules and Solids, Springer-Verlag, Berlin, 1995.
[4] J.P. Perdew, J.A. Chevary, S.H. Vosko, K.A. Jackson, M.R. Pederson, D.J. Singh, C. Fiolhais, Phys. Rev. B 46 (1991) 6671.
[5] Y.M. Juan, E. Kaxiras, Phys. Rev. B 48 (1993) 14944.
[6] R.M. Dreizler, E.K.U. Gross, Density Functional Theory, Springer-Verlag, Berlin, 1990.
[7] G.A. Benesh, J.E. Inglesfield, J. Phys. C: Solid State Phys. 17 (1984) 1595.
[8] D.E. Ellis, G.A. Benesh, E. Byrom, J. Appl. Phys. 49 (1978) 1543.
[9] H. Sellers, Chem. Phys. Lett. 178 (1991) 351.
[10] Y. Fukunishi, H. Nakatsuji, J. Chem. Phys. 97 (1992) 6535.
[11] J.D. Head, S.J. Silva, J. Chem. Phys. 104 (1996) 3244.
[12] H.A. Duarte, D.R. Salahub, J. Chem. Phys. 108 (1998) 743.
[13] J.L. Whitten, T.A. Pakkanen, Phys. Rev. B 21 (1980) 4357.
[14] A.B. Kunz, J.M. Vail, Phys. Rev. B 38 (1988) 1058.
[15] I.V. Abarenkov, V.L. Bulatov, R. Godby, V. Heine, M.C. Payne, P.V. Souchko, A.V. Titov, I.I. Tupitsyn, Phys. Rev. B 56 (1997) 1743.
[16] T. Wesolowski, A. Warshel, J. Phys. Chem. 97 (1993) 8050.
[17] P. Cortona, Phys. Rev. B 44 (1991) 8454.
[18] Y.A. Wang, N. Govind, E.A. Carter, in preparation.
[19] M. Dupuis, A. Marquez, E.R. Davidson, HONDO 95.3 from CHEM-Station, IBM Corporation, Neighborhood Road, Kingston, New York, NY, 1995.
[20] G.B. Bachelet, D.R. Hamann, M. Schlüter, Phys. Rev. B 26 (1982) 4199.
[21] W.J. Stephens, H. Basch, M. Krauss, J. Chem. Phys. 81 (1984) 6026.
[22] C.F. Bender, E.R. Davidson, J. Chem. Phys. 47 (1967) 4972.
[23] A Many Electron Description, originally written by L. McMurchie, S. Elbert, S. Langhoff, E.R. Davidson, and further advanced by D. Rawlings, D. Feller, Quantum Chemistry Group, Indiana University, Bloomington, IN.

[24] S.F. Boys, F. Bernardi, Mol. Phys. 19 (1970) 553.

[25] N. Govind, J.L. Mozos, H. Guo, Phys. Rev. B 51 (1995) 7101.

[26] R. Raval, S.F. Parker, M.E. Pemble, P. Hollins, J. Pritchard, M.A. Chesters, Surf. Sci. 203 (1988) 353.

[27] C.-L. Fu, K.-M. Ho, Phys. Rev. B 28 (1983) 5480.

[28] T.H. Dunning Jr., P.J. Hay, in: H.F. Schaeffer III (Ed.), Methods of Electronic Structure Theory, Vol. 2, Plenum Press, New York, NY, 1977.

[29] P.J. Hay, W.R. Wadt, J. Chem. Phys. 82 (1985) 299.

[30] F. Perrot, J. Phys.: Condens. Matter 6 (1994) 431.

[31] Q. Zhao, M. Levy, R.G. Parr, Phys. Rev. A 47 (1993) 918.

[32] P. Fuentealba, O. Reyes, Chem. Phys. Lett. 232 (1995) 31.

[33] E. Smargiassi, P.A. Madden, Phys. Rev. B 49 (1994) 5220.